Outcomes from water drop impact on hydrophobic meshes

Raziyeh Akbari [1], Wei Yu [1,2], Alberto Bagni[1], Riccardo Ruffo[1], Marie-Jean Thoraval[2], Longquan Chen (陈龙泉)[3,4,] Carlo Antonini [1,*]

[1]Department of Materials Science, University of Milano-Bicocca, via R. Cozzi 55, 20125 Milano, Italy

[2]School of Aerospace, Xi'an Jiaotong University, Xi'an 710049, P. R. China

[3]School of Physics, University of Electronic Science and Technology of China, Chengdu 610054, People's Republic of China

[4]Institute of Electronic and Information Engineering of UESTC in Guangdong, Dongguan 523808, People's Republic of China

(Received XX 2023; accepted XX 2023; published XX 2023)

Experimental method

Stainless steel meshes were used (square pore openings (l)= 80µm, wire diameter (w)= 50µm, solid fraction (Φ)= 0.62, mesh number #185, sample size= 2.5*1.5*0.005 cm^3). Wettability was tuned by electrodeposition. The sample set includes: S0, the reference un-coated mesh, S1-S3: meshes coated with Cu by electrodeposition in cyclic voltammetry mode for 1 to 3 cycles, respectively, and S4, a same electrodeposition process as S3, with additional hydrophobic treatment by silanization. Electrodeposition was performed using aqueous 0.1M $CuSO_4$ as electrolyte, Pt wire and saturated calomel electrode (SCE) as counter and reference electrodes, respectively. The potential was swept between 0 (vs. ref) and -1.2 V with a scan rate of 20 mV s^{-1}. For hydrophobization of S4, the sample was immersed in 2.2 mM 1H,1H,2H,2H-perfluorododecyltrichlorosilane (FTS) solution in hexane for 1 minutes and rinsed in hexane afterwards.

The drop impact experiments were conducted with a ~5.7 µl ($D_0 = 2.2\ mm$ in diameter) distilled water drop ($\rho = 997 \frac{Kg}{m^3}, \sigma = 72.8 \frac{mN}{m}, \mu = 1.0016\ mPa.s$), with drop velocities (U)= [0.4, 3.7] m s^{-1} and We= [6, 413]. The impact was captured using a high-speed camera (Photron Fastcam SA4) with a spatial resolution of 20 µm px^{-1} and a frame rate of 5 kfps with backlight illumination. A schematic of the drop impact set-up is represented in Figure S1a. The same optical setup was used to measure the wetting characteristics, i.e. advancing (θ_a) and receding (θ_r) contact angles, and hysteresis ($\Delta\theta$) and analyzed by Dropen software. All the wetting and impact measurements were repeated three times. A Vega TS5136 XM TESCAN was used for scanning electron microscopy (SEM) analysis.

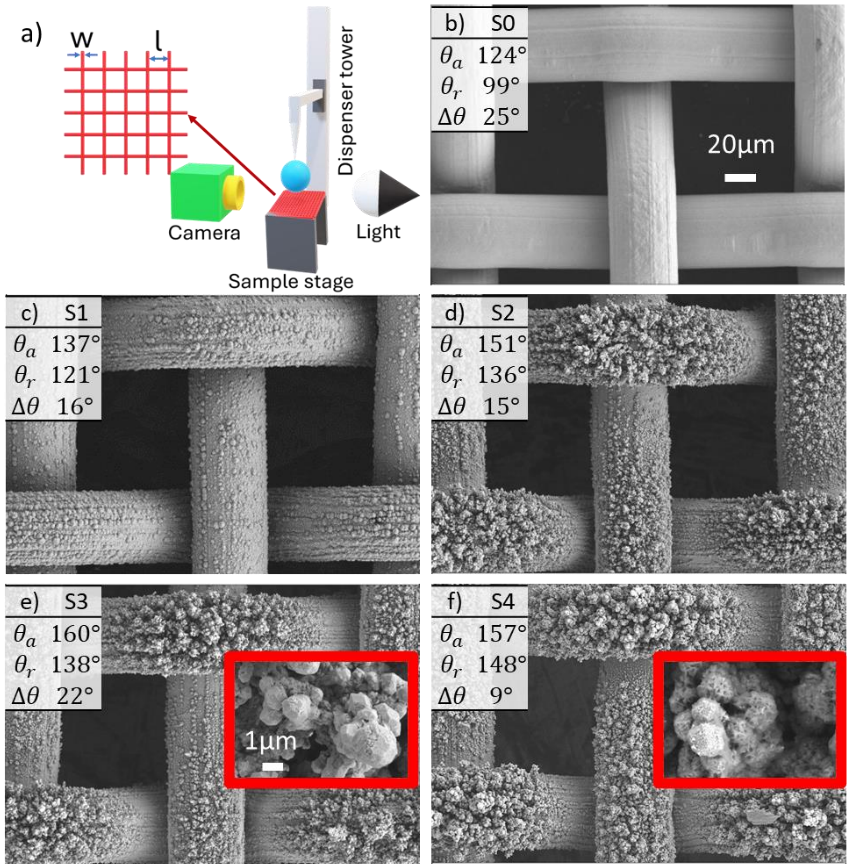

Figure S1: a) a schematic of the home-made drop impact test setup with the indication of dimensions of the mesh. b-f) SEM images along with the wetting characteristics of S0-S4 samples. Insets in e and f are magnified images of the surfaces before (S3) and after (S4) silanization. The error in the contact angle measurements is $< \pm 3°$.

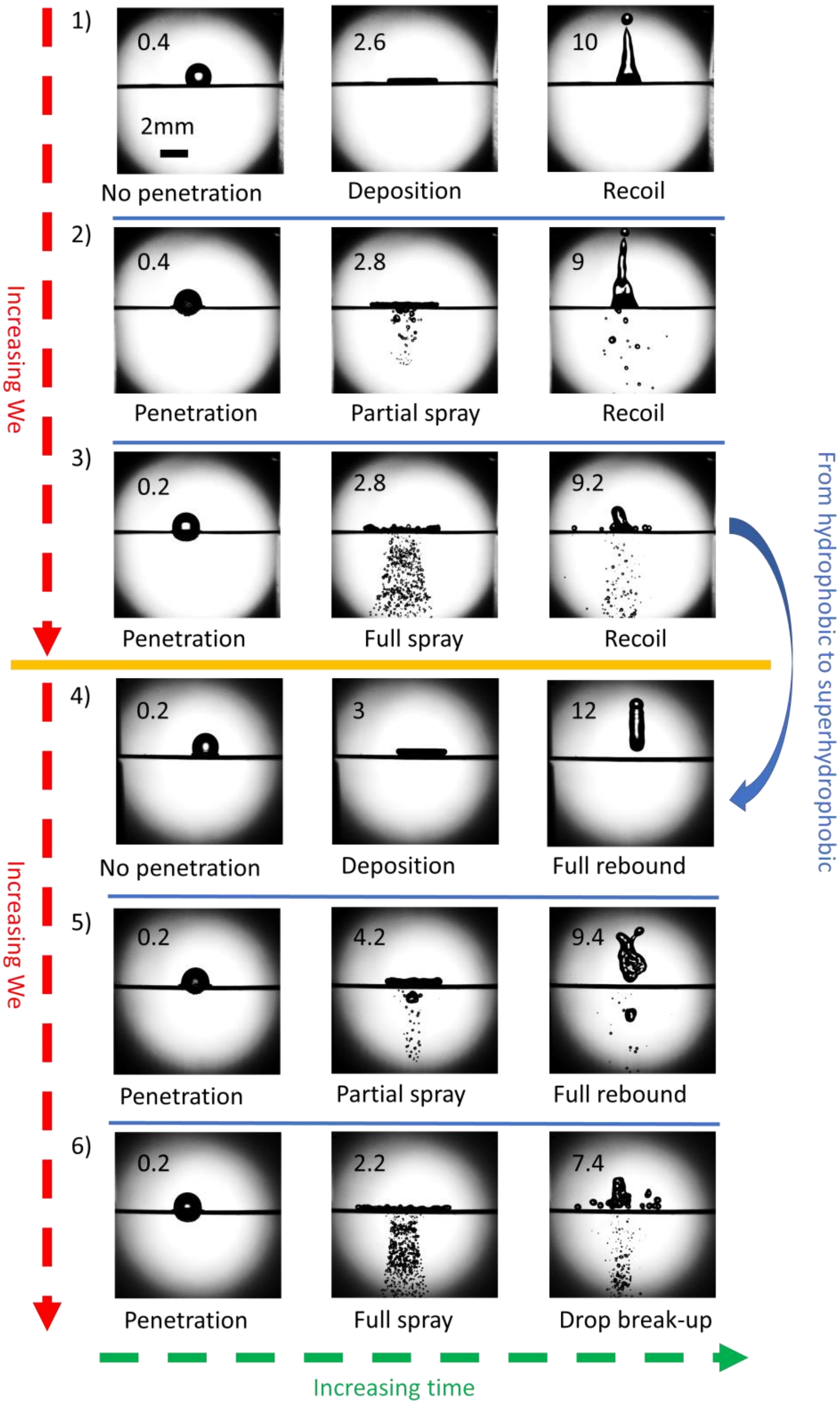

Figure S2: Representative examples of different sequences of outcomes from drop impact tests on hydrophobic and superhydrophobic meshes by increasing *We*. The event time in ms are written on each image.

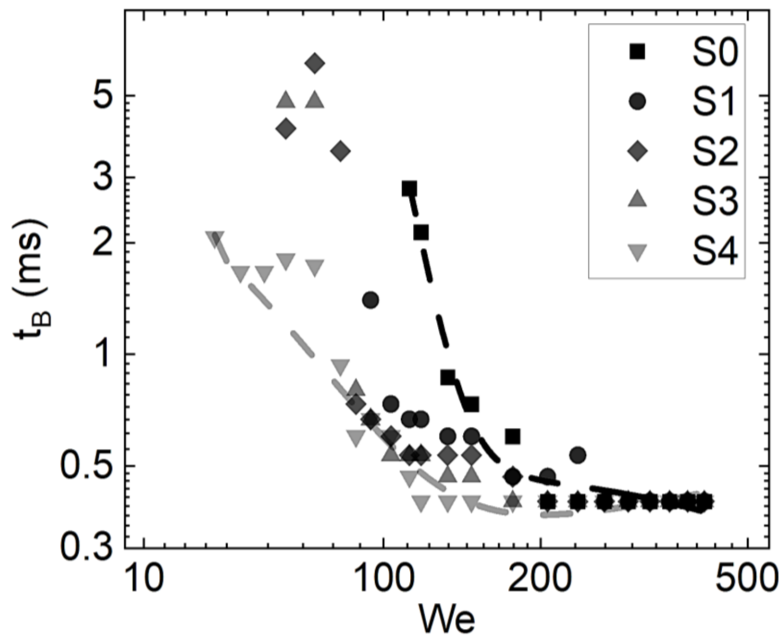

Figure S3: Droplet break time under the mesh during spraying as a variable of We. Dashed lines are for the eye guidance.

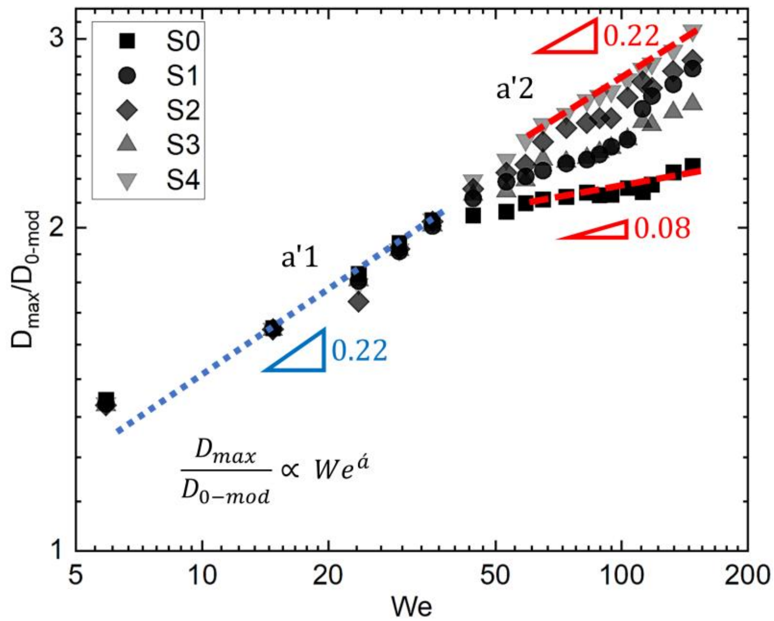

Figure S4: $D_{max}/D_{0\text{-}mod}$ vs. We. a'1 and a'2 are slopes for We< We_P~40 and We> 60, respectively. $D_{0\text{-}mod}$ is the drop initial diameter by applying the reduction in the drop volume after spraying under the mesh. The dotted blue line shows the data fitting to the power of We, written in the figure, in We<40, and the red dashed lines are the similar fitting for We>60 for S0 and S4 samples as examples. The triangles and the numbers beside them show the fitting line slopes.

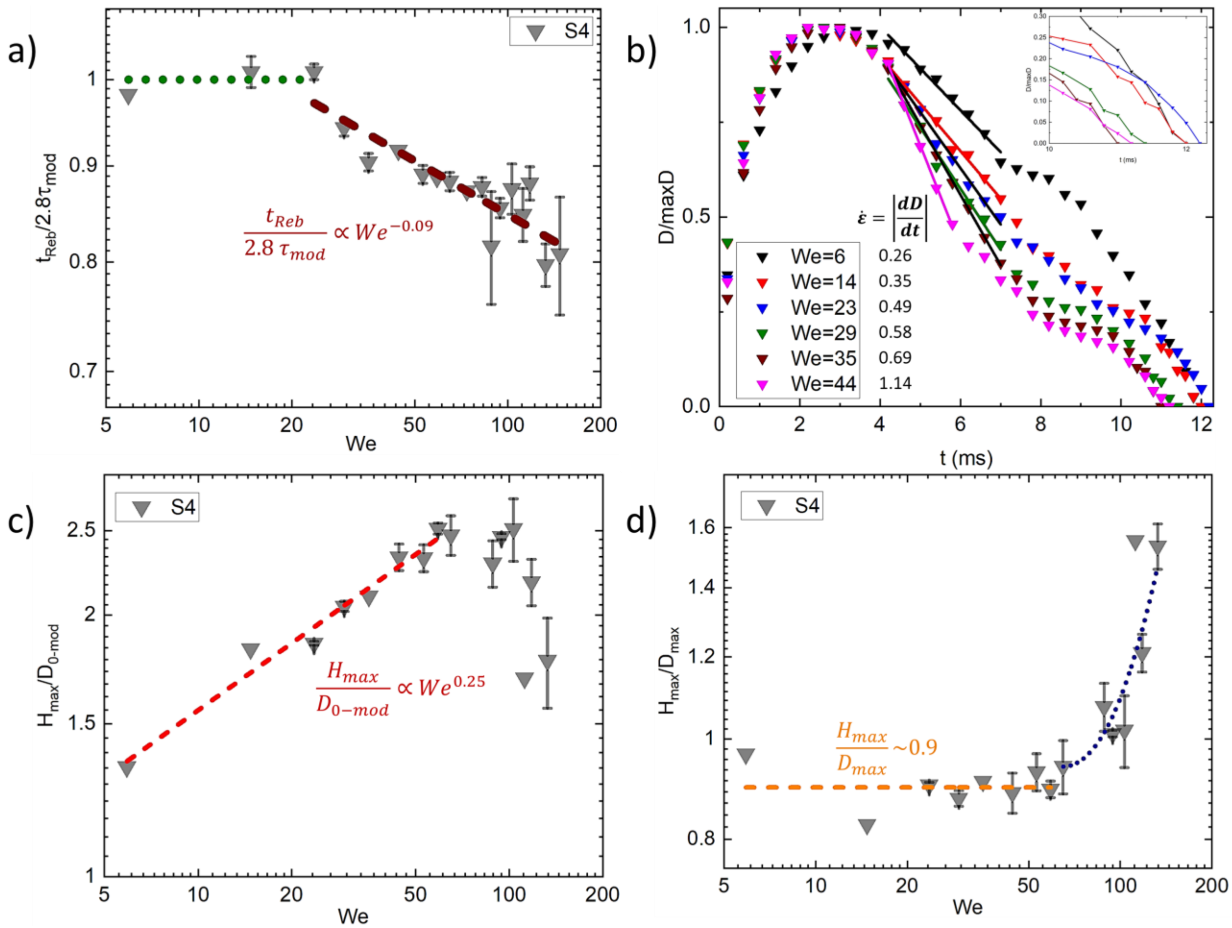

Figure S5: In S4 sample: (a) The ratio between the drop rebound time and the Rayleigh oscillation time modified by the spray volume vs. We. b) The drop contact diameter on the mesh surface during spreading and recoiling phases in We<45. maxD is the maximum contact diameter of the droplet on the mesh and solid lines correspond to the maximum retraction rate $\dot{\varepsilon}$ in ms^{-1}. A magnified figure of the drop detaching frames is presented as an inset in b. c) The bouncing drop vertical elongation ratio to the drop initial diameter modified by the spray volume vs. We. d) The bouncing drop vertical elongation ratio to the maximum drop spreading vs. We. The fitting equations are written in each plot. Lines are proportional to the fitting equations.

After modifying the drop initial volume by considering the spray volume under the mesh, a two-sided relationship between the height of the bounced droplet from the mesh surface, H_{max} , and the maximum drop diameter on the mesh during spreading, D_{max}, is practiced. As such, both the bounced drop height and the maximum spreading are increasing as $\sim We^{0.25}$ in $We < 60$, see Figure S5c and d.

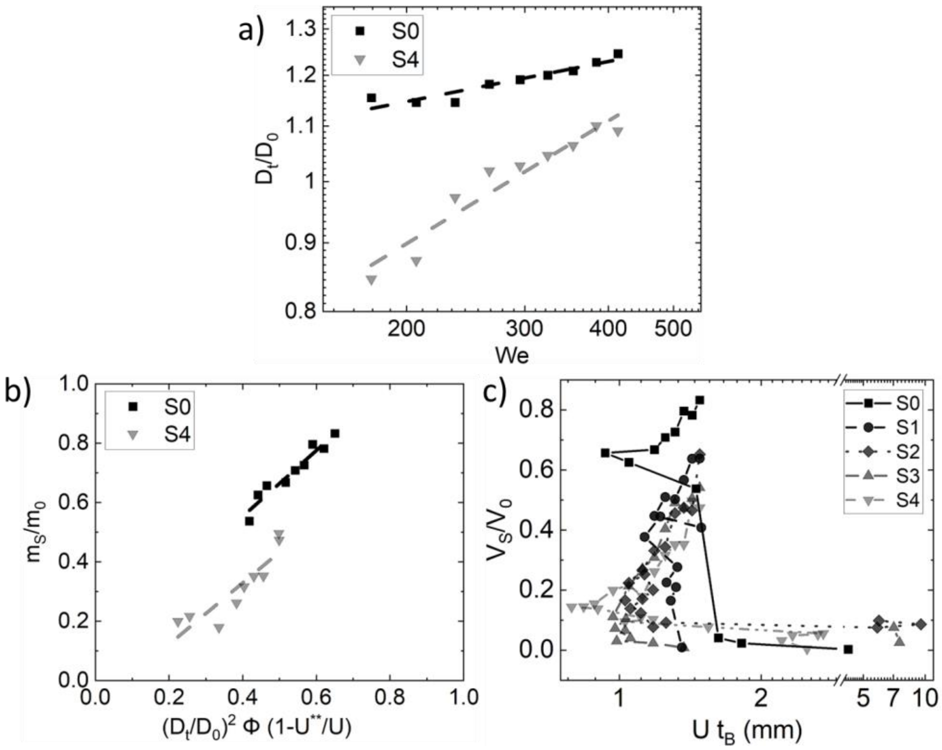

Figure S6: (a) The increase in the pore coverage Vs. We during spraying from the mesh in S0 and S4. Dashed lines shows fitting to the written equation in the figure. (b) Plotting the proposed equations for the spray mass by Soto et al. [1] and (c) for the spray volume by Kumar et al. [2]. Lines in b and c are for the eye guidance.

Soto et al. [1] developed an estimation of the increase in the spray mass, equivalent to spray volume, by increasing the drop velocity as $\frac{m_S}{m_0} \sim \left(\frac{D_t}{D_0}\right)^2 \Phi(1-\frac{U^*}{U})$, where U^* is the critical speed $2\sqrt{\frac{2\sigma}{\rho l}}$. Zong et al. [3] modified the critical penetration speed as $U^{**} = U^*\sqrt{1/(1+0.06\frac{l_c}{(l/2)})}$ by considering $l_c = \sqrt{\frac{\sigma}{\rho g}}$, the penetrating cylinder above the pore before passing through the mesh. The graph based on this equation is presented in Figure S6b and shows a linear increasing trend. Different slopes and intercepts for hydrophobic and superhydrophobic samples shows the effect of the surface wetting on the spray mass. Similarly, Kumar et al. [2] expressed that the drop final volume on the surface (V_f) which is a residue of the impacted droplet after losing the volume by spraying , bouncing off from the surface, and absorbing by the mesh, is proportional to the product of the tail velocity, equal to a ratio of the drop velocity, and the drop breaking time under the mesh, i.e. the time consuming between the impact and detachment of the liquid under the mesh, and consequently, $V_S \propto U_{tail}\, t_B$. By plotting the spray volume vs. $U_{tail}\, t_B$, Figure S6c, a step behavior depicts in the graph while there is no linear trend as proposed by Kumar.

References

[1] D. Soto, H. L. Girard, A. Le Helloco, T. Binder, D. Quéré, and K. K. Varanasi, *Droplet Fragmentation Using a Mesh*, Phys. Rev. Fluids **3**, 1 (2018).

[2] A. Kumar, A. Tripathy, Y. Nam, C. Lee, and P. Sen, *Effect of Geometrical Parameters on Rebound of Impacting Droplets on Leaky Superhydrophobic Meshes*, Soft Matter **14**, 1571 (2018).

[3] Y. Zong, A. Oron, H. Liu, and Y. Jiang, *Dynamic and Quasi-Static Droplet Penetration through Meshes*, Langmuir (2023).